HHS Public Access

Author manuscript

J Glob Antimicrob Resist. Author manuscript; available in PMC 2021 October 26.

Published in final edited form as:

J Glob Antimicrob Resist. 2020 September ; 22: 811–817. doi:10.1016/j.jgar.2020.06.023.

Nanoparticles as antibiotic-delivery vehicles (ADVs) overcome resistance by MRSA and other MDR bacterial pathogens: The grenade hypothesis

Amjed Alabresm[a,b,d], **Yung Pin Chen**[a], **Savannah Wichter-Chandler**[a], **Jamie Lead**[a,b], **Brian C. Benicewicz**[c], **Alan W. Decho**[a,*]

[a]Department of Environmental Health Sciences, Arnold School of Public Health, University of South Carolina, Columbia, SC, United States

[b]Center for Environmental Nanoscience and Risk (CENR), University of South Carolina, Columbia, SC, United States

[c]Department of Chemistry and Biochemistry, University of South Carolina, Columbia, SC, United States

[d]Department of Biological Development of Shatt Al-Arab & N. Arabian Gulf, Marine Science Centre, University of Basrah, Basrah, Iraq

Abstract

Objectives: The aim of this study was to examine how the concentrated delivery of less effective antibiotics, such as the β-lactam penicillin G, by linkage to nanoparticles (NPs), could influence the killing efficiency against various pathogenic bacteria, including methicillin-resistant *Staphylococcus aureus* (MRSA) and other multidrug resistant (MDR) strains.

Methods: The β-lactam antibiotic penicillin G (PenG) was passively sorbed to fluorescent polystyrene NPs (20 nm) that were surface-functionalized with carboxylic acid (COO^--NPs) or sulfate groups (SO_4^--NPs) to form a PenG-NP complex. Antimicrobial activities of PenG-NPs were evaluated against Gram-negative and Gram-positive bacteria, including antibiotic resistant strains. Disc diffusion, microdilution assays and live/dead staining were performed for antibacterial assessments.

Results: The results showed that bactericidal activities of PenG-NP complexes were statistically significantly ($P < 0.05$) enhanced against Gram-negative and Gram-positive strains, including MRSA and MDR strains. Fluorescence imaging verified that NPs comigrated with antibiotics throughout clear zones of MIC agar plate assays. The increased bactericidal abilities of NP-linked

*Corresponding author at: Department of Environmental Health Sciences, Arnold School of Public Health, University of South Carolina, Columbia, SC, United States, awdecho@mailbox.sc.edu (A.W. Decho).

Competing interests
The authors declare no conflict of interest.

Ethical approval
Not required.

Appendix A. Supplementary data
Supplementary data associated with this article can be found, in the online version, at https://doi.org/10.1016/j.jgar.2020.06.023.

antibiotics are hypothesized to result from the greatly increased densities of antibiotic delivered by each NP to a given bacterial cell (compared with solution concentrations of antibiotic), which overwhelms the bacterial resistance mechanism(s).

Conclusions: As a whole, PenG-NP complexation demonstrated a remarkable activity against different pathogenic bacteria, including MRSA and MDR strains. We term this the 'grenade hypothesis'. Further testing and development of this approach will provide validation of its potential usefulness for controlling antibiotic-resistant bacterial infections.

Keywords

Antibiotic; Nanoparticle; Antibiotic-resistance; Penicillin-G; MRSA; MDR

1. Introduction

Antibiotic resistance (AR) is a growing global health concern and is rapidly developing into an emerging crisis. AR infections result in increased morbidity and mortality, with more than 50,000 people annually succumbing to these infections in the United States and Europe combined [1], and result in substantial costs in clinical and community health care settings [2]. More than 2 million illnesses occur each year as a direct result of AR infections, and more people succumb to infections related to other conditions (e.g. AIDS, cancer), whose cause is complicated by AR infections [3]. The total economic cost of antibiotic resistance to the US economy, although difficult to estimate, exceeds $20 billion in additional direct health care costs, with further costs for lost productivity as high as $35 billion a year [2,4]. It is now predicted that global mortality rates will reach 10 million annually by the year 2050 and cost an estimated $35 trillion (USD) in lost economic output [2]. Many currently used antibiotics (e.g. penicillin) are becoming progressively less effective for infection treatment owing to the preponderance of resistant bacterial strains. The rise in AR has been due, in part, to the ability of bacteria to exchange genetic resistance among cells rapidly, thus enhancing the persistence of infections [5,6].

Nanoparticles (NPs) are materials that have at least one dimension in the size range of 1–100 nm [7] and are used in various sectors [8–10]. NPs are used as efficient carriers for anticancer drugs to deliver pharmaceuticals to eukaryote cells [11,12]. NP chemistry can be engineered with high specificity to produce surfaces having different types of chemical functional groups, charges and other properties [13]. This has the potential to enable large quantities of antibiotic molecules to be carried by a single NP and delivered to an infectious bacterial cell.

NPs can be engineered with fluorophores to facilitate quantitative detection [14,15]. These properties offer much potential for probing bacterial infections. We postulated that linking antimicrobial compounds to NPs may enable the development of a powerful adaptable tool to limit AR infections more efficiently. Administered antibiotics typically reach bacterial cells in solution through diffusion. Although this results in a rather homogeneous dispersion of molecules spread over tissues, it greatly reduces the concentration of antibiotic molecules reaching any given pathogenic cell involved in the infection. However, when antibiotics are concentrated on an NP surface, they can potentially deliver a more concentrated dose to

a given bacterial cell. This offers the possibility that the antimicrobial efficiencies of less effective antibiotics may be altered by their delivery to resistant bacteria using NPs.

The present study was conducted to examine how the concentrated delivery of an antibiotic (e.g. penicillin G) using NPs could influence the killing efficiency of bacterial pathogens, even strains that exhibit relatively strong resistance to the antibiotic. Polystyrene NPs were specifically chosen for use in this study because they are nonbiodegradable [16] over the time-scale of the study, their fluorescence facilitates quantification [17,18], and their sizes (diameter) were highly consistent [19]. This allowed us to use them as antibiotic carriers in a repeatable manner for our study.

2. Materials and methods

2.1. Nanoparticles

The NPs used in this study were obtained from Molecular Probes (Thermo Fisher Scientific, Waltham, MA). They consisted of fluorescent spheres with a constant polystyrene core composition, but which varied in the type of surface functionalization (Supplementary Table S1):

1. Surface-functionalized carboxylate-nanoparticles (COO^--NPs) were size-estimated by transmission electron microscopy (TEM) and exhibited fluorescence (excitation/emission [excit/emiss] = 575/620 nm).

   The NPs had relatively high densities (ca. 3290/NP) of (pendent) carboxylic acids on their surfaces (Sigma Chemical, Mumbai, India) and were relatively hydrophilic.

2. Surface-functionalized sulfate NPs (SO_4^--NPs) contained ca. 2540 pendent sites per NP, were relatively hydrophobic, enabling passive sorption of almost any protein (pK_a 2), and exhibited fluorescence (excit/emiss = 485/528 nm). Zeta potentials (mV) of NPs were measured using a ZetaPALS Zeta-Potential Analyzer (Brookhaven Instruments, Holtsville, NY).

These NPs were used in previous studies for their efficient fluorescence yield, purity and uniformity of size [20–23]. NPs were detected and quantified based on fluorescence emissions, with conversions to concentration determined using calibration curves. Three replicates per treatment time were used for each time course measurement. The core sizes of the NPs were verified using transmission electron microscopy (TEM).

2.2. Antibiotic

The antibiotic penicillin G potassium salt (Supplementary Fig. S1; Fisher Scientific) benzylpenicillin or Pen G. Concentrations of bound versus unbound Pen G were quantified by absorbance (220 nm) using spectrophotometry (UV-Vis spectrophotometer, Shimadzu, Tokyo).

2.3. Linking antibiotics to nanoparticles

To link Pen G to NPs, 20 μL/mL of carboxylated NPs or sulfated NPs and 1 mg Pen G were added to 1 mL deionised (DI) water, mixed well and incubated at 28 °C with gentle shaking (50 rpm/min.). Centrifugal ultrafiltration (Amicon Ultra-0.5 tubes, 3000 MWCO, Invitrogen, Thermo Fisher Scientific; 10,000 rpm; 10 min) was used to separate freely dissolved Pen G from Pen G–NP complexes. Finally, the NP–Pen G complexes were recovered from the centrifuged ultrafiltration device and placed into a clean microcentrifuge tube for 2 min, 1000 rpm, 4 °C. The concentrated complexes were suspended into 1 mL of DI water and stored at 4 °C until further use.

The optimum times for incubation for Pen G–NP complexes were analyzed by calculating the amount of free Pen G in supernatant using an ultraviolet (UV) spectrophotometric method after determining traction times (0, 1, 2, 3 and 4 h). Complexes of bound versus unbound Pen G were quantified using UV spectrophotometry at an absorbance of 220 nm (UV-Vis; Shimadzu, Tokyo). NPs were quantified by fluorescence by constructing standard calibration curves. All measurements were determined in triplicate. Optimal associations of Pen G to NPs occurred after a 3-h incubation, which was used for all further experimental incubations.

2.4. Transmission electron microscopy

The morphology of the NPs was analyzed with TEM (Hitachi, HT7800, Tokyo). The NPs were sonicated using VWR Ultrasonic Cleaner (power, 220 W; frequency, 60 MHz; VWR International, Radnor, PA) for 20 min and then deposited on PELCO® TEM 200 mesh copper grids with Formvar/carbon support films (Ted Pella, Redding, CA) and dried in a hood for 10 min prior to TEM observations.

2.5. Antimicrobial activity assay of Pen G–NPs

The antimicrobial activities of Pen G–NPs, Pen G and NPs were evaluated against Gram-negative and Gram-positive bacteria, including antibiotic-resistant strains. Gram-negative bacteria used were *Pseudomonas aeruginosa* ATCC 27853, *Klebsiella pneumoniae* ATCC 27736, *Salmonella typhimurium* (ATCC 13311) and *Proteus vulgaris* (ATCC 33420). The Gram-positive strains tested were *Staphylococcus aureus* ATCC 25423 and several additional MRSA strains.

Antibiotic resistance was also tested against several MDR strains: *Escherichia coli* (BAA-197); MRSA-252 (ATCC BAA-1720); a community isolate CA-MRSA strain (ATCC-BAA 1717); a hospital isolate HA-MRSA strain (ATCC BAA-29213); and an antibiotic-sensitive strain (methicillin-susceptible *Staphylococcus aureus* [MSSA], ATCC BAA-1718), which is resistant to penicillin. Bacterial strains were cultured in tryptic soy broth (TSB) overnight and then stored in 25% glycerol at −80 °C until use.

2.6. Antibacterial assessments using two approaches

Disc diffusion assays: The disc diffusion method, as described in Clinical and Laboratory Standards Institute (CLSI) guideline M100S, was used to determine the bioactivity of Pen G–NPs, Pen G and NPs against the various pathogens mentioned earlier. Briefly, plates were

prepared using 10 mL tryptic soy agar (TSA) into sterile Petri dishes (9 cm) and allowed to set. The TSA medium plates were spread evenly with 100 μL of an overnight log culture of the test organism. Sterile paper discs (6 mm diameter) were placed on each plate. Then, 25 μL containing known concentrations of Pen G–NPs, Pen G or NPs was added to each disc and incubated at 37 °C for 24 h. Inhibition zones around the disc were measured. MICs for all tested pathogens were calculated using standard protocols by measuring the depth and diameter of clear zones on the agar after incubation [24]. The MIC was defined as the lowest concentration of an antimicrobial agent (μg/mL) required to inhibit bacterial growth after an overnight incubation when compared with a negative control [25].

Microdilution method: MICs of Pen G–NPs, Pen G and NPs were determined against the bacterial strains according to standard methods of the National Committee for Clinical Laboratory Standards (NCCLS) [24]. For all microdilution assays, 96-well plates were used to determine the MICs of Pen G and the two forms of NP–Pen G (i.e. using carboxylated NPs and sulfated NPs) as antibiotic carriers. Using seed cultures of each bacterial strain and 200 μL of TSB broth, a range of Pen G (0.5–30 μg) was added to each well. The same concentrations of Pen G–NPs were also added to separate wells. All MIC determinations were run in triplicate.

2.7. Monitoring diffusion of nanoparticles

To determine if the Pen G remained associated with their NP carrier, the corresponding diffusion of NPs and clear zones due to antibiotic were measured. Plates were prepared as previously described for the disc diffusion method. Then, 25 μL of Pen G–NP, Pen G and NPs was added to each disc and incubated (37 °C for 24 h). The diffusion of Pen G–NPs and its corresponding antibacterial activity were determined by measuring the diameters of the fluorescence (by NPs) and the inhibition zones surrounding the discs, respectively.

3. Results

3.1. Nanoparticles and determination of Pen G–NP complexes

Sizes of the NPs were confirmed to be 22–24 nm for carboxylated NPs and 23–24 nm for sulfated NPs, as determined using TEM (Fig. 1). The average zeta potential was 40.2 ± 1.7 mV for carboxylated NPs and 36.0 ± 0.6 mV for sulfated NPs (Supplementary Table S1).

The complexation of Pen G to NPs occurred relatively rapidly (i.e. <1 h) after the addition of NPs to Pen G in solution. Fig. 2A shows that concentrations (measured by absorbance at 220 nm) of unbound Pen G in the supernatant (after centrifugation) decreased, whereas concentrations of the Pen G–NP complex in the pellet fraction increased over time. The Pen G–NP complex reached an optimum complexation after 4 h of incubation. The formation of Pen G–NP complexes were followed by absorbance measurements. Fig. 2B shows that the absorption spectra of Pen G has a λ_{max} of 230 nm. However, the absorption of the Pen G–NP complex was completely changed and indicated that a new complex was formed. Furthermore, after initial scanning of absorbance between 245 and 800 nm with a UV-Vis double-beam spectrophotometer, the same λ_{max} (230 nm) was observed in both soluble Pen G and the Pen G–NP complex. This was likely due to the linking of Pen G to NPs. TEM

images showed that there was no detectable change in the size or shape of NPs after Pen G sorption. The NPs remained spherical and of similar size as uncoated NPs.

3.2. Antimicrobial potential of Pen G–NP complexes

The antimicrobial activities of Pen G, NPs and Pen G–NPs were tested against Gram-negative, Gram-positive and AR bacteria. The results showed that MIC values of several bacterial strains were significantly reduced ($P < 0.05$ by ANOVA), compared with controls, when Pen G was complexed to sulfated or carboxylated NPs. These included the strains of *Pseudomonas aeruginosa* (ATCC 27853), *Proteus vulgaris* (ATCC 33420), *Salmonella typhimurium* (ATCC 13311) and *Klebsiella pneumoniae* (ATCC 27736). A next step was to test both types of Pen G–NP complexes against specific pathogen bacterial strains that are known to possess resistance mechanisms against Pen G. When Pen G bound to NPs was administered at a relatively low concentration, it was effective against MRSA strains, even though the same concentration of Pen G in solution form was ineffective (Table 1). These strains included *Escherichia coli* (BAA-197), a hospital-acquired MRSA-252 (ATCC BAA-1720) strain and a community-acquired MRSA (BAA-1717) strain, all MDR strains. Table 1 shows the results of NP-antibiotic complex activities and the corresponding MICs for several bacterial strains (see Supplementary Figs. S2–S4). Moreover, the effectiveness of the sulfated NPs, carboxylated NPs and Pen G alone was screened by the disc diffusion assay with their zones of inhibition against CA-MSSA, HA-MRSA and MRSA-252, as shown in Fig. 3. Results showed that the Pen G alone (control) has no effect on these strains, as was expected, whereas significant zones of inhibition were found for both Pen G–NPs complexes against CA-MSSA, and intermediate inhibition zones were detected against CA-MSSA and HA-MRSA.

4. Discussion

Examples of NP applications as antimicrobial agents are emerging rapidly in the literature. The inherent antimicrobial properties of certain NPs such as silver and other metals is well documented [26–31]. The application of NPs as delivery vehicles for antimicrobial molecules such as antibiotics is now being realized and offers promise [32]. This promise, coupled with the emergence of multiple AR bacterial strains [33–36] and a concurrent reduction in the discovery of new antibiotics [37–39], has prompted the study of NP applications [40]. In addition, the reapplications of older, less effective antibiotics is also being studied [41].

The present study shows that the complexation of the traditional antibiotic Pen G with NPs results in significantly greater killing efficacies of bacterial pathogens, including those that are resistant to Pen G, and also MDR strains. Results of Pen G, NPs and Pen G–-NPs, when tested against several strains of Gram-negative and Gram-positive bacteria, showed that MIC values were significantly reduced ($P < 0.05$ by ANOVA), compared with controls, when Pen G was complexed to sulfated or carboxylated NPs. The bacterial strains were those of the common pathogens *P. aeruginosa* (ATCC 27853), *P. vulgaris* (ATCC 33420), *S. typhimurium* (ATCC 13311) and *K. pneumoniae* (ATCC 27736) (Table 1).

The diffusion of fluorescent NP-linked antibiotics and NPs alone were compared over the 24-h time frames used in the MIC plate assays. The results indicated that NPs alone were unable to diffuse in the agar plates as determined by fluorescence (data not shown). However, when Pen G was sorbed to NPs, they were able to diffuse throughout the cleared zones of MIC plates. This indicated that the NPs accompanied—that is, i.e. remained complexed to—antibiotics during the killing of bacteria throughout the cleared zones on MIC plates.

When MDR strains were tested, a similar pattern was observed for NP-complexed antibiotics. When Pen G bound to NPs was administered at relatively low concentrations, effective antimicrobial activities were measured against MRSA strains, even though the same concentration of Pen G in solution form was ineffective (Table 1). These strains included *E. coli* (BAA-197), a hospital-acquired MRSA-252 (ATCC BAA-1720) strain, and a community-acquired MRSA (BAA-1717) strain, all MDR strains. Pen G, when bound to NPs, displayed significantly greater antibacterial activities against resistant forms of MSSA, MRSA and other pathogenic bacterial strains (Fig. 3), whereas the soluble Pen G at the same concentrations were less active or completely inactive against the same respective strains. NP-only controls (with no added antibiotic present) did not inhibit bacterial strains. Using the disc diffusion assay as a screening method, the sulfated NPs and carboxylated NPs showed inhibitory activity against CA-MSSA, HA-MRSA and MRSA-252, but the Pen G alone had no observable zones of inhibition against these strains. The linkage of Pen G with NPs may actually be advantageous for antimicrobial activity because a microorganism may have difficulty in recognizing new compounds that act synergistically against the target organism.

Many MDR bacterial strains secrete β-lactamases, which are enzymes that specifically degrade Pen G and other β-lactam antibiotics, rendering the strain resistant. The β-lactam ring represents a central moiety of the core structure of several families of β-lactam antibiotics, such as penicillin, cephalosporins, carbapenems and monobactams. Nearly all these antibiotics work by inhibiting bacterial cell wall biosynthesis, which is an ongoing process in most bacteria [42]. Interference with cell wall biosynthesis by β-lactams results in lethal effects on bacteria, but concurrently propagates the emergence of sub-groups (already present in populations) that are resistant to β-lactam antibiotics.

Penicillin is generally considered as a less effective bactericide against Gram-negative cells, when compared with Gram-positives due to the protective outer membrane of the former [43]. In our study the Gram-negative strains that we tested were resistant to soluble Pen G. Interestingly, however, these same Gram-negative strains were significantly inhibited when Pen G was complexed to NPs. β-Lactams invoke their bacteriostatic properties by acting as nonfunctional analogues for naturally occurring penicillin-binding proteins (PBPs). This group of enzymes is critical to cross-linking the peptidoglycan of bacterial cell walls [44]. The inhibition by NP-associated Pen G suggests that NP delivery of this antibiotic overcame membrane barriers and penicillin-binding protein defences, such as PBP2, of these Gram-negative bacteria.

Antibiotics or drugs loading onto NPs can be used as a novel approach to delivery. This is an attempt to develop a new mechanism to overcome strong pathogens, including MDR bacteria, and to determine the efficacy and potential for therapeutic applications.

4.1. Grenade hypothesis of NP delivery of antibiotics

Our results suggest that complexation of antibiotics with NP carriers could be developed as a novel approach for overcoming resistance to hydrolysis by β-lactamases. The widespread use of β-lactam antibiotics, primarily against Gram-positives, has led to the emergence of resistant microbial strains, with enhanced production of β-lactamase enzymes. Many genes for β-lactamase production, and over 1800 different molecular forms of these enzymes, have now been identified [45]. Therefore, altering the potential susceptibility to hydrolysis of β-lactam-type antibiotics requires further study to increase the activity of these drugs.

Many Pen G molecules potentially can be sorbed to a single NP. Therefore, a single NP, once in contact with the bacterial cell, would deliver a relatively large dose (i.e. pulse) of Pen G molecules to that cell when compared with the same concentration of Pen G molecules administered in solution form and homogeneously diffusing throughout the local medium near a cell. We posit that an antibiotic complexed to a given NP could be delivered at a very high localized concentration to that cell. This high localized concentration has the capability to overwhelm the cell's inherent AR defences, such as β-lactamases, capabilities for rapid efflux pumps and other potential defences [13,46–48]. The concentration experienced by a given cell in contact with an antibiotic-NP complex will be many times greater than the cell would experience from the same antibiotic in solution because the latter is homogenously dispersed via diffusion.

The absorption spectra of soluble Pen G (220 nm = λ_{max}) was modified with complexation to NPs and exhibited a new accessory peak for NP–Pen G complex (570 nm = λ_{max}). This was likely due to the surface modification induced by the sorption of the Pen G to NPs when compared with NP controls.

Fig. 4 (graphical abstract) outlines the simple complexation of many Pen G molecules to the surface of a NP, which has the net result of increasing antimicrobial activity to a bacterial cell. Based on the present results, we hypothesize that NP delivery of this protects the β-lactam antibiotic from hydrolysis (by β-lactamases) and then releases sufficient (i.e. enough to kill) concentrations of Pen G molecules to overwhelm the outer membrane and cell wall defences. The complexation of Pen G to the NP might also provide a camouflage to protect the β-lactam ring from β-lactamase-mediated hydrolyses and retain the activity of PenG. How this might occur at a molecular level, however, remains to be determined.

Supplementary Material

Refer to Web version on PubMed Central for supplementary material.

Funding

This work was supported by grants from the US National Science Foundation [BME-1608151], National Institutes of Health NIAID [RO1 AI120987], University of South Carolina ASPIRE Program and Center for Environmental

Nanoscience and Risk (CENR) in the Arnold School of Public Health at the University of South Carolina. B.C.B. and J.R.L. also acknowledge support by the South Carolina Smart State Chair Program.

References

[1]. Centers for Disease Control and Prevention. The drug push. American Association for the Advancement of Science; 2015.

[2]. Centers for Disease Control and Prevention. Antibiotic resistance threats in the United States. Washington, DC: CDC; 2013.

[3]. Centers for Disease Control and Prevention. Antibiotic use in the United States: progress and opportunities. 2017 https://www.cdc.gov/antibiotic-use/stewardship-report/pdf/stewardship-report.pdf8.

[4]. Ventola CL. The antibiotic resistance crisis: part 1: causes and threats. Pharm Ther 2015;40(4):277.

[5]. Andam CP, Fournier GP, Gogarten JP. Multilevel populations and the evolution of antibiotic resistance through horizontal gene transfer. FEMS Microbiol Rev 2011;35:756–67, doi:10.1111/j.1574-6976.2011.00274.x. [PubMed: 21521245]

[6]. Martínez JL, Rojo F. Metabolic regulation of antibiotic resistance. FEMS Microbiol Rev 2011;35:768–89, doi:10.1111/j.1574-6976.2011.00282.x. [PubMed: 21645016]

[7]. Batista CAS, Larson RG, Kotov NA. Nonadditivity of nanoparticle interactions. Science 2015;350:1242477, doi:10.1126/science.1242477. [PubMed: 26450215]

[8]. Alabresm A, Mirshahghassemi S, Chandler GT, Decho AW, Lead J. Use of PVP-coated magnetite nanoparticles to ameliorate oil toxicity to an estuarine meiobenthic copepod and stimulate the growth of oil-degrading bacteria. Environ Sci: Nano 2017, doi:10.1039/C7EN00257B.

[9]. Alabresm A, Chen YP, Decho AW, Lead J. A novel method for the synergistic remediation of oil-water mixtures using nanoparticles and oil-degrading bacteria. Sci Total Environ 2018;630:1292–7, doi:10.1016/j.scitotenv.2018.02.277. [PubMed: 29554750]

[10]. Cao X, Alabresm A, Chen YP, Decho AW, Lead J. Improved metal remediation using a combined bacterial and nanoscience approach. Sci Total Environ 2019;135378, doi:10.1016/j.scitotenv.2019.135378. [PubMed: 31806322]

[11]. Kumar A, Mansour HM, Friedman A, Blough ER. Nanomedicine in drug delivery. Boca Raton, FL: CRC Press; 2013.

[12]. Lundqvist M, Stigler J, Elia G, Lynch I, Cedervall T, Dawson KA. Nanoparticle size and surface properties determine the protein corona with possible implications for biological impacts. Proc Natl Acad Sci U S A 2008;105:14265–70, doi: 10.1073/pnas.0805135105. [PubMed: 18809927]

[13]. Wang L, Chen YP, Miller KP, Cash BM, Jones S, Glenn S, et al. Functionalised nanoparticles complexed with antibiotic efficiently kill MRSA and other bacteria. Chem Commun 2014;50:12030–3, doi:10.1039/C4CC04936E.

[14]. Kim CK, Ghosh P, Pagliuca C, Zhu Z-J, Menichetti S, Rotello VM. Entrapment of hydrophobic drugs in nanoparticle monolayers with efficient release into cancer cells. J Am Chem Soc 2009;131:1360–1, doi:10.1021/ja808137c. [PubMed: 19133720]

[15]. Baptista PV, McCusker MP, Carvalho A, Ferreira DA, Mohan NM, Martins M, et al. Nano-strategies to fight multidrug resistant bacteria—"A Battle of the Titans". Front Microbiol 2018;9:1441, doi:10.3389/fmicb.2018.01441. [PubMed: 30013539]

[16]. Frohlich E Cellular targets and mechanisms in the cytotoxic action of nonbiodegradable engineered nanoparticles. Curr. Drug Metab 2013;14(9):976–88. [PubMed: 24160294]

[17]. Ranganathan A, Campo J, Myerson J, Shuvaev V, Zern B, Muzykantov V, et al. Fluorescence microscopy imaging calibration for quantifying nanocarrier binding to cells during shear flow exposure. J Biomed Nanotechnol 2017;13:737–45. [PubMed: 29104516]

[18]. Strungaru S-A, Jijie R, Nicoara M, Plavan G, Faggio CC. Micro-(nano) plastics in freshwater ecosystems: abundance, toxicological impact and quantification methodology. Trends Analyt Chem 2019;110:116–28.

[19]. Gagné F, Auclair J, André C. Polystyrene nanoparticles induce anisotropic effects in subcellular fraction of the digestive system of freshwater mussels. Currr Top Toxicol 2019;15:43–9.

[20]. Bloem J, Veninga M, Shepherd J. Fully automatic determination of soil bacterium numbers, cell volumes, and frequencies of dividing cells by confocal laser scanning microscopy and image analysis. Appl Environ Microbiol 1995;61:926–36. [PubMed: 16534976]

[21]. Kolodny LA, Willard DM, Carillo LL, Nelson MW, Van Orden A. Spatially correlated fluorescence/AFM of individual nanosized particles and biomolecules. Anal Chem 2001;73(9):1959–66, doi:10.1021/ac001472z. [PubMed: 11354476]

[22]. Lai SK, O'Hanlon DE, Harrold S, Man ST, Wang Y-Y, Cone R, et al. Rapid transport of large polymeric nanoparticles in fresh undiluted human mucus. Proc Natl Acad Sci U S A 2007;104:1482–7, doi:10.1073/pnas.0608611104. [PubMed: 17244708]

[23]. Nevius BA, Chen YP, Ferry JL, Decho AW. Surface-functionalization effects on uptake of fluorescent polystyrene nanoparticles by model biofilms. Ecotoxicology 2012;21:2205–13, doi:10.1007/s10646-012-0975-3. [PubMed: 22806556]

[24]. Wiegand I, Hilpert K, Hancock REW. Agar and broth dilution methods to determine the minimal inhibitory concentration (MIC) of antimicrobial substances. Nat Protoc 2008;3:163–75, doi:10.1038/nprot.2007.521. [PubMed: 18274517]

[25]. Andrews JM. Determination of minimum inhibitory concentrations. J Antimicrob Chemother 2001;48(Suppl 1):5–16, doi:10.1093/jac/48.suppl_1.5. [PubMed: 11420333]

[26]. Kim JS, Kuk E, Yu KN, Kim J-H, Park SJ, Lee HJ, et al. Antimicrobial effects of silver nanoparticles. Nanomedicine 2007;3:95–101, doi:10.1016/j.nano.2006.12.001. [PubMed: 17379174]

[27]. Horie M, Fujita K, Kato H, Endoh S, Nishio K, Komaba LK, et al. Association of the physical and chemical properties and the cytotoxicity of metal oxide nanoparticles: metal ion release, adsorption ability and specific surface area. Metallomics 2012;4:350–60, doi:10.1039/C2MT20016C. [PubMed: 22419205]

[28]. Ivask A, Elbadawy A, Kaweeteerawat C, Boren D, Fischer H, Ji Z, et al. Toxicity mechanisms in Escherichia coli vary for silver nanoparticles and differ from ionic silver. ACS Nano 2014;8:374–86, doi:10.1021/nn4044047. [PubMed: 24341736]

[29]. Fabrega J, Renshaw JC, Lead JR. Interactions of silver nanoparticles with *Pseudomonas putida* biofilms. Environ Sci Technol 2009;43:9004–9, doi:10.1021/es901706. [PubMed: 19943680]

[30]. Fabrega J, Fawcett SR, Renshaw JC, Lead JR. Silver nanoparticle impact on bacterial growth: effect of pH, concentration, and organic matter. Environ Sci Technol 2009;43:7285–90, doi:10.1021/es803259g. [PubMed: 19848135]

[31]. Fabrega J, Zhang R, Renshaw JC, Liu W-T, Lead JR. Impact of silver nanoparticles on natural marine biofilm bacteria. Chemosphere 2011;85:961–6, doi:10.1016/j.chemosphere.2011.06.066. [PubMed: 21782209]

[32]. Hussein-Al-Ali SH, El Zowalaty ME, Hussein MZ, Geilich BM, Webster TJ. Synthesis, characterization, and antimicrobial activity of an ampicillin-conjugated magnetic nanoantibiotic for medical applications. Int J Nanomed 2014;9:3801, doi:10.2147/IJN.S61143.

[33]. Klevens RM, Morrison MA, Nadle J, Petit S, Gershman K, Ray S, et al. Invasive methicillin-resistant *Staphylococcus aureus* infections in the United States. JAMA 2007;298:1763–71. [PubMed: 17940231]

[34]. Boucher HW, Talbot GH, Bradley JS, Edwards JE, Gilbert D, Rice LB, et al. Bad bugs, no drugs: no ESKAPE! An update from the Infectious Diseases Society of America. Clin Infect Dis 2009;48:1–12, doi:10.1086/595011. [PubMed: 19035777]

[35]. Andersson DI, Hughes D. Antibiotic resistance and its cost: is it possible to reverse resistance? Nat Rev Microbiol 2010;8(4):260, doi:10.1038/nrmicro2319. [PubMed: 20208551]

[36]. Khan SN, Khan AU. Breaking the spell: combating multidrug resistant 'superbugs'. Front Microbiol 2016;7:174. [PubMed: 26925046]

[37]. Wenzel RP. The antibiotic pipeline—challenges, costs, and values. N Engl J Med 2004;351:523–6. [PubMed: 15295041]

[38]. Pelaez F The historical delivery of antibiotics from microbial natural products—can history repeat? Biochem Pharmacol 2006;71:981–90, doi: 10.1016/j.bcp.2005.10.010. [PubMed: 16290171]

[39]. Demain AL, Sanchez S. Microbial drug discovery: 80 years of progress. J Antibiot 2009;62:5, doi:10.1038/ja.2008.16.

[40]. Greene S, Reid A. Moving targets: fighting the evolution of resistance in infections, pests, and cancer. 2013 https://www.asmscience.org/content/report/colloquia/colloquia.32.

[41]. Cassir N, Rolain J-M, Brouqui P. A new strategy to fight antimicrobial resistance: the revival of old antibiotics. Front Microbiol 2014;5:551, doi: 10.3389/fmicb.2014.00551. [PubMed: 25368610]

[42]. Park JT, Uehara T. How bacteria consume their own exoskeletons (turnover and recycling of cell wall peptidoglycan). Microbiol Mol Biol Rev 2008;72:211–27, doi:10.1128/MMBR.00027-07. [PubMed: 18535144]

[43]. Fischetti VA. Bacteriophage lytic enzymes: novel anti-infectives. Trends Microbiol 2005;13:491–6, doi:10.1016/j.chemosphere.2011.06.066. [PubMed: 16125935]

[44]. Tipper DJ, Strominger JL. Mechanism of action of penicillins: a proposal based on their structural similarity to acyl-d-alanyl-d-alanine. Proc Natl Acad Sci U S A 1965;54:1133, doi:10.1073/pnas.54.4.1133. [PubMed: 5219821]

[45]. Brandt C, Braun SD, Stein C, Slickers P, Ehricht R, Pletz MW, et al. In silico serine β-lactamases analysis reveals a huge potential resistome in environmental and pathogenic species. Sci Rep 2017;7:43232, doi:10.1038/srep43232. [PubMed: 28233789]

[46]. Ganapthy ME, Huang W, Rajan DP, Carter AL, Sugawara M, Iseki K, et al. β-Lactam antibiotics as substrates for OCTN2, an organic cation/carnitine transporter. J Biol Chem 2000;275:1699–707, doi:10.1074/jbc.275.3.1699. [PubMed: 10636865]

[47]. Nikaido H, Pagès J-M. Broad-specificity efflux pumps and their role in multidrug resistance of Gram-negative bacteria. FEMS Microbiol Rev 2012;36:340–63, doi:10.1111/j.1574-6976.2011.00290.x. [PubMed: 21707670]

[48]. Brown AN, Smith K, Samuels TA, Lu J, Obare SO, Scott ME. Nanoparticles functionalized with ampicillin destroy multiple-antibiotic-resistant isolates of *Pseudomonas aeruginosa* and *Enterobacter aerogenes* and methicillin-resistant *Staphylococcus aureus*. Appl Environ Microbiol 2012;78:2768–74, doi:10.1128/AEM.06513-11. [PubMed: 22286985]

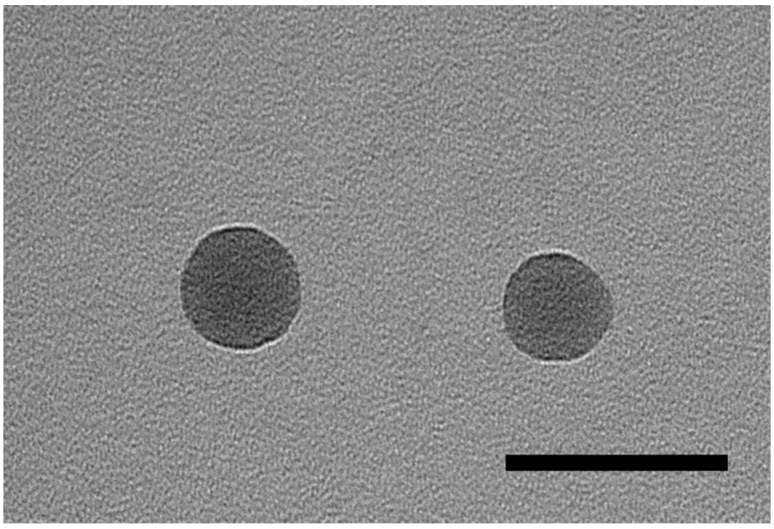

Fig. 1.

Transmission electron microscopy (TEM) micrograph showing polystyrene surface-functionalized carboxylate nanoparticles (NPs; 23–24 nm) used in experiments (scale bar = 50 nm).

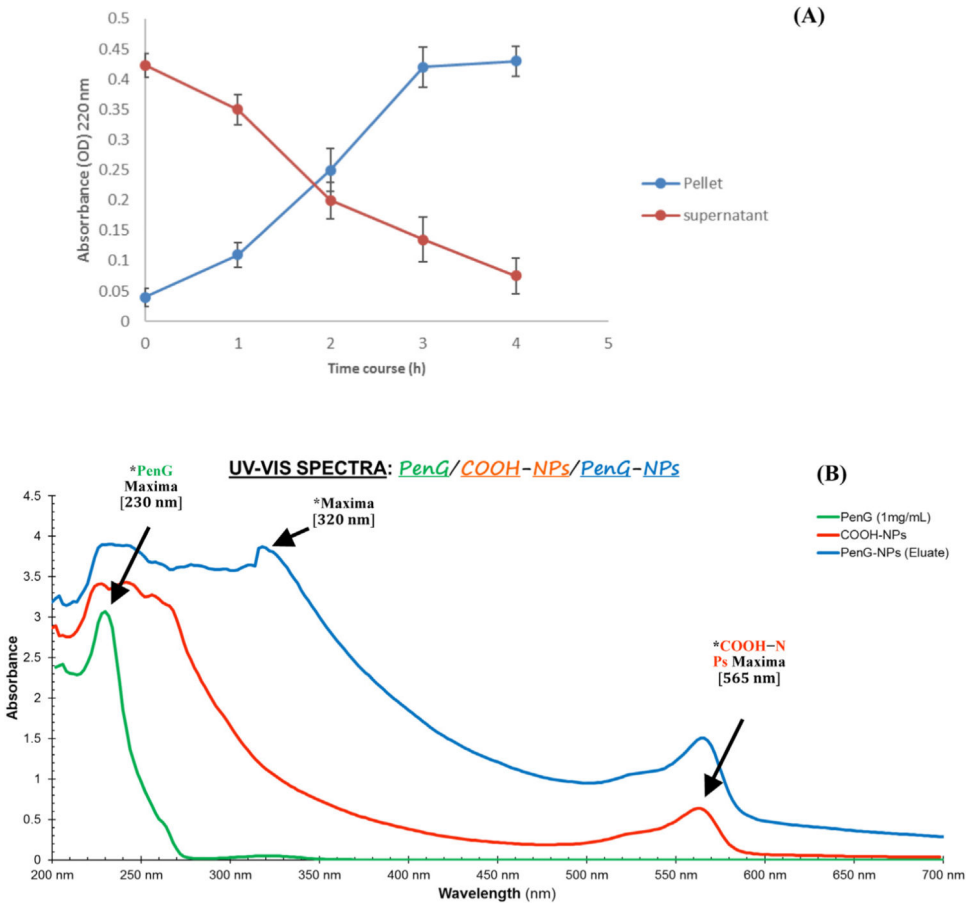

Fig. 2.

(A) Complexation of penicillin G (PenG) to nanoparticle (NP) carrier versus time. The red line shows corresponding decrease in PenG in solution measured by absorbance (230 nm). The blue line shows that the formation of the carboxylated NP–PenG complex (detected in pellet after centrifugation) increased over time. (B) Shown is the ultraviolet (UV) visible spectrum of PenG, carboxylated NPs (C-NPs) and PenG–carboxylated NP complex (C-NPs-PenG).

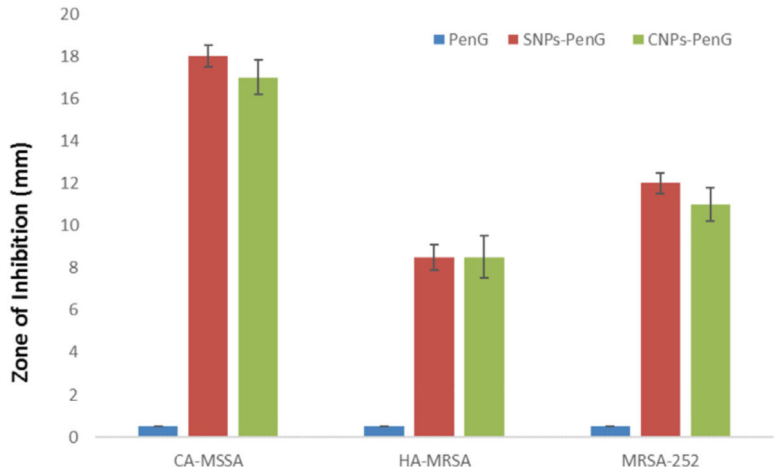

Fig. 3.

Antimicrobial activity of penicillin G (PenG), SNP–PenG complex and CNPs–PenG complex against CA-MSSA, HA-MRSA and MRSA-252, CNPs, Carboxylated nanoparticles (NPs); SNPs, sulfated NPs.

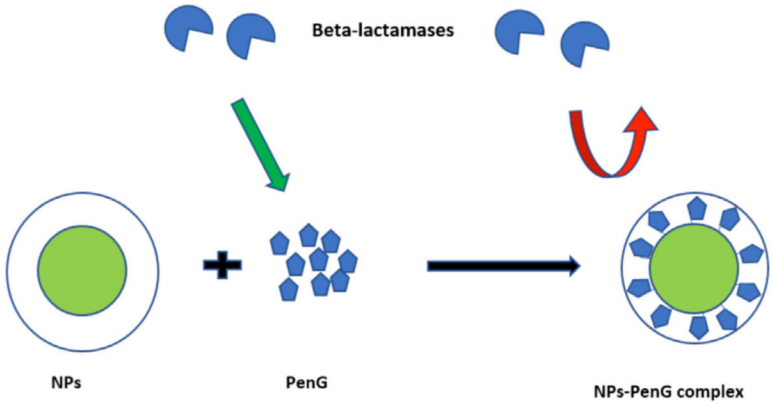

Fig. 4.

Schematic illustration showing the hydrolysis of free penicillin G (PenG) by β-lactamases and protection against β-lactamase by the PenG–nanoparticles (NPs) complex.

J Glob Antimicrob Resist. Author manuscript; available in PMC 2021 October 26.

Table 1

Results of nanoparticle (NP)–antibiotic complex experiments.[a]

Bacterial pathogen strain	ATCC strain no.	Minimum inhibitory concentration, μg/mL							
		Control Pen G (soluble)	SD	Sulfated NPs	SD	Improvement (%)	Carboxylated NPs	SD	Improvement (%)
Escherichia coli	BAA-197	17.5	3	11.9[b]	0.5	32	12[b]	0.6	31
Pseudomonas aeruginosa	27853	24.9	2	16.8[b]	0.9	33	15.2[b]	1	39
Salmonella typhimurium	13311	15.7	5	4.5[b]	0.7	71	4[b]	0.2	75
Proteus vulgaris	33420	16.8	5	6.4[b]	0.7	62	5.8[b]	0.2	65
Klebsiella pneumoniae	27736	28.3	2	15[b]	0.9	47	13.6[b]	0.4	52
Staphylococcus aureus	25423	10	2	5[b]	0.5	50	5[b]	0.6	50
MRSA-252 (MDR)	BAA-1720	>100 (ND)	–	12.1[b]	0.5	88	20.5[b]	2	80
CA-MRSA (MDR)	BAA-1717	38.6	8	18.9[b]	1	51	17[b]	0.8	56
HA-MRSA	29213	12.6	4	8.3[b]	0.3	34	6.7[b]	0.7	47
MSSA	BAA-1718	16.5	3	5.5[b]	0.4	67	4[b]	0.4	76

[a]These show minimum inhibitory concentrations (MICs) for each bacterial strain tested. Valúes represent mean ± standard deviation (SD) ($n = 3$).

[b]Indicates that the treatment is significantly different ($P < 0.05$) from the control (penicillin G).MDR, multidrug-resistant; MRSA, methicillin-resistant *Staphylococcus aureus;* MSSA, methicillin-susceptible *Staphylococcus aureus.*